ACTA IMEKO
ISSN: 2221-870X
September 2026, Volume 15, Number 3, 1 - 7

In-situ molecular investigation of ancient and restoration mortars from the theatre of Tindari (Sicily, Italy) by DRIFTS and µ-Raman spectroscopy

Giuseppe Paladini[1], Francesco Caridi[1], Domenico Majolino[1], Gabriele Lando[2], Paola Cardiano[2], Valentina Venuti[1]

[1] *Department of Mathematical and Computer Sciences, Physical Sciences and Earth Sciences, University of Messina, Viale F. Stagno d'Alcontres 31, 98166 Messina, Italy*
[2] *Department of Chemical, Biological, Pharmaceutical and Environmental Sciences, University of Messina, Viale F. Stagno d'Alcontres 31, 98166 Messina, Italy*

ABSTRACT
We report an in-situ multi-technique study combining Diffuse Reflectance Infrared Fourier Transform Spectroscopy (DRIFTS) and µ-Raman spectroscopy for the molecular characterization of five mortar areas from the theatre of Tindari (Sicily, Italy). The selected areas, chosen as representative case studies within a broader diagnostic campaign, include three ancient mortars attributed to the Roman transformation phase of the monument, and two modern conglomerate- and cement-based materials employed in restoration works. The ancient areas are located on the podium and on the intrados of the vault of the annular corridor encircling the orchestra, while the modern restoration mortars are located on the *scaena*. DRIFTS spectra provided information averaged over the superficial portion investigated, whereas µ-Raman spectroscopy allowed the analysis of individual grains and localized phases. The analyses revealed clear compositional differences among the investigated mortars, mainly involving quartz-, calcite-, clay-rich, and cement-related phases, together with Raman markers deriving from carotenoid (beta-carotene)-containing biological colonization. The comparison between DRIFTS and µ-Raman data demonstrates the complementarity of the two techniques for rapid in situ screening of heterogeneous historical mortars. In particular, DRIFTS rapidly characterizes the overall molecular composition, whereas µ-Raman resolves individual mineral constituents and localized alteration products. Noteworthy, the identification of mineral phases, restoration materials, and biodeterioration markers provides a valuable basis for targeted analytical investigations and informed conservation planning.

Section: RESEARCH PAPER

Keywords: DRIFTS; µ-Raman spectroscopy; ancient mortars; Tindari theatre; conservation

Citation: G. Paladini, F. Caridi, D. Majolino, G. Lando, P. Cardiano, V. Venuti, In-situ molecular investigation of ancient and restoration mortars from the theatre of Tindari (Sicily, Italy) by DRIFTS and µ-Raman spectroscopy, Acta IMEKO, vol. 15 (2026) no. 3, pp. 1-7. DOI: 10.21014/actaimeko.v15i3.2350

Section Editor: Fabio Leccese, Università Degli Studi Roma Tre, Rome, Italy

Received March 23, 2026; **In final form** September 11, 2026; **Published** September 2026

Funding: This research activity was funded by the European Union (NextGeneration EU), through the MUR-PNRR project SAMOTHRACE (ECS00000022) "SiciliAn MicronanOTecH Research And Innovation CEnter" – Ecosistema dell'innovazione (PNRR, Mission 4, Component 2 Investment 1.5, Avviso n. 3277 del 30-12-2021), Spoke 2 – University of Messina – Work Package 6 Cultural Heritage.

Corresponding author: Paola Cardiano, e-mail: pcardiano@unime.it

1. INTRODUCTION

The theatre of Tindari (Sicily, Italy) is a Hellenistic monument that dominates the archaeological area from a promontory overlooking the Tyrrhenian Sea (Figure 1). Over the centuries, the building has been repeatedly adapted and restored, both in the antiquity and in the modern era, to maintain its use as a venue for performances and cultural events.

Numerous studies have dealt with the architectural layout, construction history and stylistic features of the monument [1], [2], whereas only a limited number of works explicitly address its conservation state and degradation processes currently affecting it [3]. Previous restoration and reconstruction activities, often involving the introduction of modern materials, are documented particularly for the period 1938–1965 [4], [5]. As a consequence, original masonry and twentieth-century repairs coexist, and the identification of ancient mortars, as well as the assessment of

Figure 1. The Theatre of Tindari (Sicily, Italy).

their long-term behaviour, becomes crucial for designing compatible conservation strategies.

Multi-analytical approaches combining spectroscopic and chemical techniques have been increasingly applied to investigate construction materials, such as mortars [6]–[11]. These methodologies provide insights into raw material selection, production technology, and conservation strategies. For instance, Marcaida et al. [12] characterized mortars and tesserae from Pompeii mosaics using non-invasive techniques, while Gómez-Laserna et al. [13] investigated the impact of environmental conditions on building materials in coastal areas. Similar integrated studies on Roman structures have been reported by Couvidat et al. [14], which highlight the contribution of such analyses to assess ancient artificial material formulations in view of designing compatible, modern mortars. Going on, an example of the application of mineralogical and petrographic approaches for the characterization of lime mortars was provided by D. Pereira da Silva Dalto et al. [15], which employed integrated analytical methods (commonly including optical microscopy and phase identification methods) for the assessment of the compositional and textural features of natural and anthropogenic materials, essential in the view of reconstructing raw material provenance, understanding production technologies, and evaluating long-term durability. Recently, S. Spoto et al. [11] conducted a comprehensive investigation of plasters and mortars from the Church of the Annunciation in Tortorici (Messina, Italy), through X-ray fluorescence (XRF) and Raman spectroscopy, to identify the materials' composition and degradation patterns for building vulnerability assessments.

Within this broader framework, the theatre of Tindari represents an interesting case study due to its complex construction history and exposure to a marine environment, where salt-laden winds, temperature excursions, and moisture variations may enhance decay processes. A detailed molecular characterization of mortars belonging to different parts of the building can contribute to reconstruct ancient technological strategies, and to better understand the response of these materials to environmental agents.

In this context, mortar fragments belonging to different phases were selected based on visual inspection and analysed at the molecular scale by DRIFTS and μ-Raman spectroscopy, with the aim of characterizing both ancient and modern restored areas of the theatre [4], [5]. The selection of the areas investigated in the present work was supported by a parallel archaeological and architectural reassessment of the monument carried out within the SAMOTHRACE project. This reassessment included a new survey of the theatre, a technical reading of the standing structures, a preliminary distinction of the building phases, and the integration of stratigraphic information into a dedicated GIS [16], [17].

In this study, five locations were selected on the monument: three ancient mortars attributed to the Roman transformation phase of the theatre, and two modern restoration mortars. The ancient mortars come from the podium and from the vaulted annular corridor that surrounds the orchestra, while the modern mortars were selected from restored areas of the *scaena*. These five locations are representative case studies selected from a broader in-situ diagnostic campaign; therefore, the results should be considered preliminary and mainly aimed at evaluating the potential of the combined DRIFTS/μ-Raman approach for mortar analysis and diagnostics.

The use of DRIFTS and μ-Raman spectroscopy is particularly advantageous in this context: both techniques are non-destructive, require minimal or no sampling, and can be implemented in-situ with portable instrumentation, making their combined application highly effective for discriminating between different mineralogical phases and for identifying subtle variations in mortar composition.

Based on that, we aim to:

(i) characterize the main mineralogical phases of both ancient and restoration mortars from the theatre of Tindari;
(ii) compare ancient mortars with modern repair mortars to assess compositional and textural differences relevant to structural function and restoration history;
(iii) evaluate the capabilities and limitations of the integrated DRIFTS/μ-Raman approach as a non-destructive diagnostic tool to support conservation strategies for monumental archaeological sites.

2. MATERIALS AND METHODS

As a part of a broader diagnostic campaign, 25 locations were selected on the monument for in-situ spectroscopic measurements. The chosen points are distributed over the scenic building and the *cavea*, to sample different construction elements and restoration zones. Each location was documented by photographs that record both the wider context and the exact area probed by the instruments. At least one spectroscopic measurement was taken at every point, ensuring that the analyzed spot was representative of the mortar texture visible to the naked eye.

In this paper, five areas are discussed in detail (Figure 2): three ancient mortars attributed to one specific Roman transformation phase of the monument, and two modern restoration mortars. Therefore, the ancient dataset considered here does not represent the full chronological complexity of the theatre or all ancient construction phases. In particular, TY_OU_9 and TY_OU_19 are ancient mortars from the podium, whereas TY_OU_10 was analysed on the intrados of the vault of the annular corridor encircling the orchestra. According to the archaeological and architectural reassessment of the monument, the annular corridor belongs to Phase IV of the current phasing, corresponding to the Roman transformation of the theatre for *venationes*. At present, a more specific absolute chronology cannot yet be assigned to this phase. In addition, TY_OU_1 and

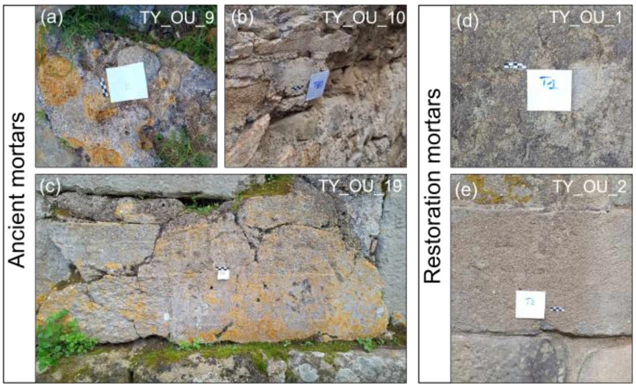

Figure 2. Different investigated areas representative of (a-c) ancient (i.e. TY_OU_9 (from the podium), TY_OU_10 (from the vault), TY_OU_19 (from the podium)), and (d,e) modern (i.e. TY_OU_1 (conglomerate) and TY_OU_2 (cement)) mortars. See text for details.

TY_OU_2, a conglomerate and a cement mortar, respectively, are located on different sides of the *scaena* and are representative of modern restoration materials.

2.1. DRIFTS measurements

DRIFTS measurements were carried out using a 4300 Topscan hand-held FTIR spectrometer (Agilent) equipped with a diffuse reflectance sampling interface. Spectra were acquired in the 650–4000 cm^{-1} range at a spectral resolution of 4 cm^{-1}, collecting 32 scans for each measurement. The spot size on the surface was about 2 mm in diameter. The system is equipped with a ZnSe beamsplitter and a DTGS detector. A diffuse gold cap was used as the reference for background measurements, which were frequently repeated during the survey to check for instrumental drift and variations in environmental conditions. No baseline correction was applied to the whole raw dataset. Reflectance spectra have been then converted to pseudo-absorbance through the employment of the Agilent MicroLab software. For proper interpretation of the DRIFTS profiles, spectra have been compared with data from literature [12], [18], [19].

2.2. μ-Raman measurements

μ-Raman measurements were obtained with a portable BTR111 MiniRam™ spectrometer (BW&TEK Inc.), operating with a 785 nm excitation wavelength and a thermoelectrically cooled CCD detector. The system was equipped with a BAC151B Raman microscope. The laser spot was focused through an 80 × objective, providing a working distance of 1.24 mm and a laser beam spot size of 25 μm. Spectra were recorded between 60 and 3150 cm^{-1}, using a spectral resolution of 8 cm^{-1} and an acquisition time of 40 s; 32 accumulations were collected to improve the signal-to-noise ratio. Spectra were collected from several spots, targeting visually distinct micro areas (different in colour, grain size, and compactness) identified on the surface of each fragment under optical inspection prior to analysis.

To avoid localized overheating and surface degradation, the laser power at the sample surface was kept within the range of 10–30 mW. Band assignment was based on comparison with reference spectra from databases and literature [20]–[22].

3. RESULTS AND DISCUSSION

Figure 3 shows representative DRIFTS spectra collected on the investigated ancient mortars, i.e. the TY_OU_9, TY_OU_10

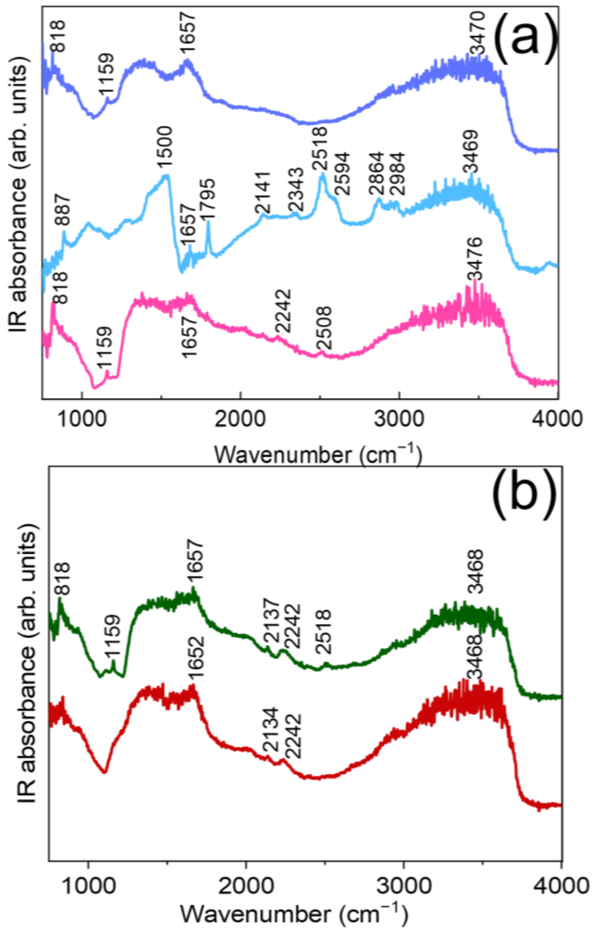

Figure 3. DRIFTS spectra collected on the investigated (a) ancient, i.e. TY_OU_9 (from the podium, pink line), TY_OU_10 (from the vault, light-blue line), and TY_OU_19 (from the podium, purple line), and (b) modern, i.e. TY_OU_1 (conglomerate, red line) and TY_OU_2 (cement, dark green line) areas in the wavenumber range between 750 cm^{-1} and 4000 cm^{-1}. Spectra were vertically offset for clarity.

and TY_OU_19 areas, and modern conglomerate- and cement-based materials, i.e. the TY_OU_1 and TY_OU_2 areas, in the 750–4000 cm^{-1} range.

As far as the ancient mortars are concerned (Figure 3a), an inspection of the spectral profiles highlights a remarkable differentiation in.. the molecular composition between samples located in the podium with respect to that in the vault. In particular, those collected from the podium (TY_OU_9 and TY_OU_19) turned out to share a common molecular signature, with strong absorption features related to the presence of quartz (SiO_2), with characteristic bands at ~818 cm^{-1} and ~1159 cm^{-1}, kaolinite ($Al_2Si_2O_5(OH)_4$), with a band at around ~1657 cm^{-1}, and water molecules within the mineral lattice and/or deriving from adsorbed moisture, with the broad feature centred at ~3470 cm^{-1}. Such spectral pattern suggests that a similar recipe was used for both areas, indicating a common manufacturing technique characteristic of a specific construction phase, possibly based on siliceous aggregates mixed with a clay-bearing binder [23]. Interestingly, only in the case of TY_OU_9, minor traces of organic compounds and calcite ($CaCO_3$) were detected, evidenced by low-intensity contributions centred at ~2242 cm^{-1} and ~2508 cm^{-1}, respectively. The weak band associated to calcite may be related to the presence of a carbonate binder or to secondary carbonate precipitation within pores, induced by weathering processes. Interestingly, the local heterogeneity of the area (likely related to the presence of clay-rich domains), as well as matrix and particle size effects, should be considered as responsible of the observed weak intensity of such spectral feature. Going on, the possible presence of organic signals might suggest the use of additives (e.g. vegetal or animal-based admixtures) or biological contamination/surface contamination within the surface [24], [25], although further analyses would be needed to confirm this hypothesis.

In contrast, the DRIFTS spectrum of TY_OU_10 exhibits a molecular signature mainly characterized by the presence of calcite ($CaCO_3$), with characteristic bands at ~1795 cm^{-1}, ~2141 cm^{-1}, ~2343 cm^{-1}, ~2518 cm^{-1}, ~2594 cm^{-1}, ~2864 cm^{-1}, and ~2984 cm^{-1} [12], [18], [19]. Worthy of note, no clear spectral features associated with quartz (SiO_2) were observed within the detection limits of the technique. However, the presence of kaolinite ($Al_2Si_2O_5(OH)_4$) (band at ~1657 cm^{-1}) and water within the crystal lattice (from the observation of the hydroxyl-related vibration at ~3469 cm^{-1}), were identified. These DRIFTS results indicate that the molecular composition of TY_OU_10 is predominantly calcite-based, suggesting the use of lime as a binder and possibly carbonate aggregates [26]. The absence of detectable quartz (SiO_2), despite the relatively large measurement area (2 mm diameter), may indicate the use of minimal sand or other siliceous aggregates. Considering the archaeological attribution of TY_OU_10 to the intrados of the annular corridor vault and of TY_OU_9/TY_OU_19 to the podium, such differences may reflect different construction choices within architecturally distinct parts of the Roman transformation phase. However, they cannot be interpreted as definitive evidence of functional differentiation without further petrographic, stratigraphic, and mechanical investigations.

DRIFTS profiles collected on modern conglomerate- and cement-based materials (Figure 3b), i.e. TY_OU_1 and TY_OU_2, showed weak signals associated to the presence of calcite ($CaCO_3$) in both areas, with characteristic bands at ~2134 cm^{-1}, ~2242 cm^{-1}, and ~2518 cm^{-1} (not visible in TY_OU_1), alongside with those related to kaolinite ($Al_2Si_2O_5(OH)_4$) (~1652 cm^{-1}) and water molecules within the crystal lattice (~3468 cm^{-1}). Interestingly, only for TY_OU_2, spectral features related to quartz (SiO_2) were identified, through the detection of its major contribution at ~818 cm^{-1} and ~1159 cm^{-1} (see the dark green profile in Figure 3b), likely reflecting the incorporation of siliceous aggregates/sand fractions within the conglomerate matrix, which are commonly employed in modern cement-based formulations [27].

Figure 4 reports the most representative µ-Raman spectra collected on different spots (Spot #, with # = 1,.., 3) of the ancient , i.e. TY_OU_9, TY_OU_10, TY_OU_19, and modern, i.e. TY_OU_1 and TY_OU_2, fragments, in the 100–2000 cm^{-1} range.

As far as the ancient mortars are concerned, a first comparison of obtained spectra (Figure 4a–c) revealed the presence, in all fragments, of all the prominent peaks corresponding to quartz (SiO_2), falling at ~129 cm^{-1}, ~205 cm^{-1}, ~357 cm^{-1}, ~465 cm^{-1}, ~808 cm^{-1}, and ~1155 cm^{-1}, with varying relative intensity reflecting both differences in the local concentration of siliceous aggregates within the mortar matrix, the size of the crystalline domains, and the crystallographic orientation of individual quartz grains with respect to the incident laser. Besides, the presence of calcite ($CaCO_3$) grains was also recognized by the prominent symmetric stretching band at ~1084 cm^{-1}, along with minor contributions at ~158 cm^{-1}, ~280 cm^{-1}, and ~710 cm^{-1}. The identification of $CaCO_3$ by µ-Raman in all ancient mortars complements the DRIFTS results and reflects the different spatial scale of the two techniques: µ-

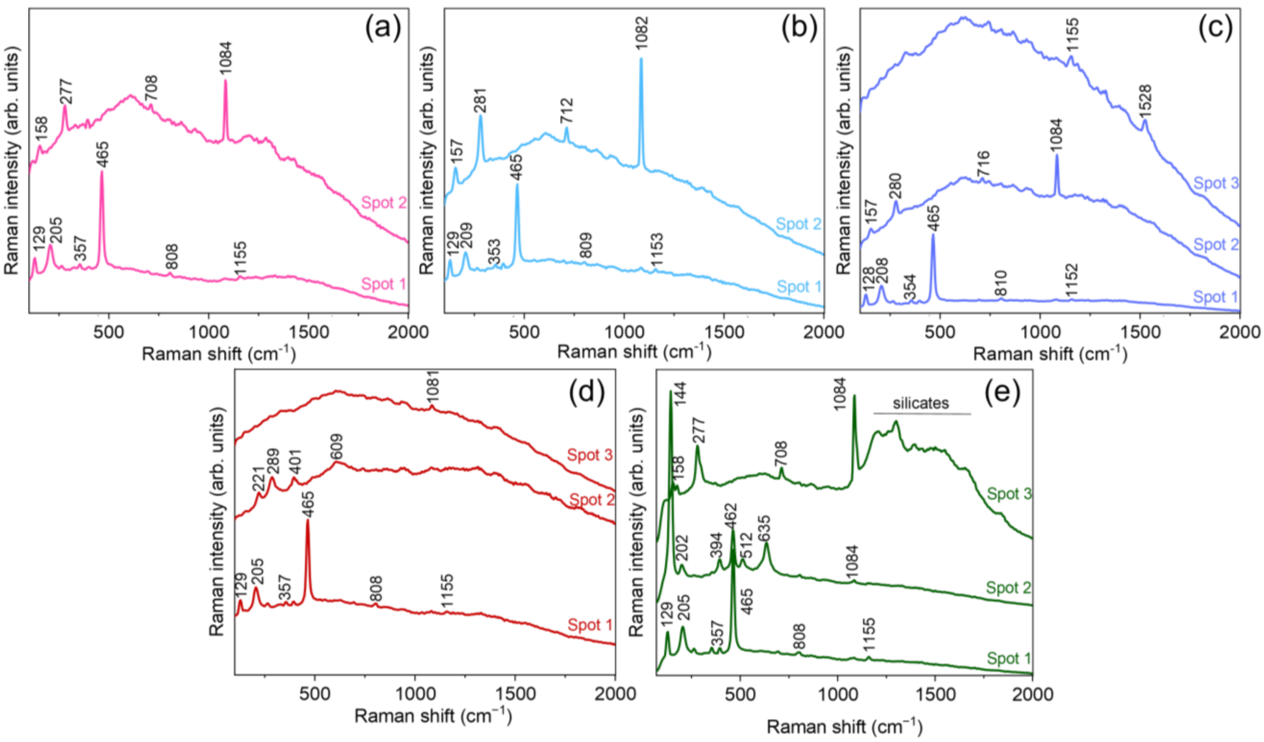

Figure 4. Comparison of the most representative µ-Raman spectra collected on different spots of the ancient, i.e. (a) TY_OU_9 (from the podium), (b) TY_OU_10 (from the vault), (c) TY_OU_19 (from the podium), and modern, i.e. (d) TY_OU_1 (conglomerate) and (e) TY_OU_2 (cement), fragments, in the wavenumber range between 100 cm^{-1} and 2000 cm^{-1}. Spectra were vertically offset for clarity.

Raman can selectively probe individual carbonate grains, whereas DRIFTS averages the response of a larger superficial area. This confirms the presence of siliceous aggregates even in TY_OU_10, where DRIFTS did not reveal clear quartz-related signals, again highlighting the complementary character of the two techniques.

Interestingly, only in the case of TY_OU_19, the presence of the two carotenoid (β-carotene) spectral bands, centered at ~1155 cm^{-1} and ~1528 cm^{-1} (Spot 3 profile in Figure 4c) are consistent with carotenoid (beta-carotene) commonly reported in cyanobacteria and phototrophic biofilms [28]–[32]—presumably of the *Gloeocapsa* species [33]. On this basis, such Raman markers and the green biofilm visible by naked eye suggest the presence of cyanobacteria-like colonization; however, taxonomic attribution to *Gloeocapsa* remains tentative without microbiological analysis. Such endolithic microorganisms, capable of forming biodeteriorative colonies depending on the species and environmental conditions [33]–[35], can be considered as responsible for the thick green biofilms covering localized areas of TY_OU_19 (see Figure 2c). By absorbing sunlight and growing endolithically, these microorganisms play a key role in the expansion and contraction of mortar surfaces, ultimately leading to biodegradation patterns associated with microboring [36], [37].

The μ-Raman analysis of the modern conglomerate- and cement-based materials (see Figure 4d–e) furnished evidence of a complex molecular scenario characterized by a mixture of several compounds. In particular, concerning the conglomerate mortar fragment (TY_OU_1, see Figure 4d), a molecular composition mainly based on quartz (SiO_2) and calcite ($CaCO_3$), from the detection of Raman bands at ~129 cm^{-1}, ~205 cm^{-1}, ~357 cm^{-1}, ~465 cm^{-1}, ~808 cm^{-1}, and ~1155 cm^{-1} (see μ-Raman profile of Spot 1 in Figure 4d), and ~1081 cm^{-1} (see μ-Raman profile of Spot 3 in Figure 4d), respectively, can be recognized, alongside with contributions falling at ~221 cm^{-1}, ~289 cm^{-1}, ~401 cm^{-1}, and ~609 cm^{-1}, all ascribable to hematite (Fe_2O_3) (see μ-Raman profile of Spot 2 in Figure 4d). The coexistence of quartz (SiO_2) and calcite ($CaCO_3$) is consistent with a typical conglomerate mortar composition, where siliceous aggregates are embedded within a carbonate-rich binder [38]. Interestingly, the detection of hematite in TY_OU_1 can be interpreted as a local feature compatible with iron-bearing grains or raw materials commonly occurring in cementitious or conglomerate formulations [39]–[41].

As far as the cement mortar is also concerned, μ-Raman profiles collected on different spots of the surface (TY_OU_2, see Figure 4e) revealed the presence of calcite (bands at 158 cm^{-1}, ~277 cm^{-1}, ~708 cm^{-1}, and ~1084 cm^{-1}, see μ-Raman profile of Spot 3 in Figure 4e), quartz (bands at ~129 cm^{-1}, ~205 cm^{-1}, ~357 cm^{-1}, ~465 cm^{-1}, ~808 cm^{-1}, and ~1155 cm^{-1}, see μ-Raman profile of Spot 1 in Figure 4e), and titanium dioxide (TiO_2) in the anatase form (bands at ~144 cm^{-1}, ~394 cm^{-1}, ~512 cm^{-1}, and ~635 cm^{-1}, see μ-Raman profile of Spot 2 in Figure 4e). Interestingly, the μ-Raman spectrum collected on Spot 3 furnished evidence of the presence of silicate phases (feldspar or kaolinite) upon the surface, likely arranged in polymerized structures within the cement matrix [42], from the broad bands between 1100 and 1900 cm^{-1} [43]–[45].

Although the present dataset is limited to five areas, the combined interpretation of DRIFTS and μ-Raman results provides several insights:

(i) Common components vs. different proportions: DRIFTS and μ-Raman spectra collected on both ancient and modern areas revealed a common set of basic components (calcite, quartz, clay minerals), but in different proportions and possibly with different textural arrangements.

(ii) Compositional differences among architecturally distinct areas: in mortars attributed to the Roman transformation phase, the podium samples TY_OU_9 and TY_OU_19 show stronger quartz- and clay-related features than TY_OU_10. This may indicate a higher contribution of siliceous aggregates and clay-bearing fractions in the analysed superficial areas. Such components may have affected texture, workability, shrinkage behaviour, and dimensional stability during drying and ageing. The TY_OU_10 area, analysed on the intrados of the vault of the annular corridor, shows a more calcite-related signature. However, this result cannot be automatically extended to the whole load-bearing structure, since the investigated point represents the accessible superficial portion of the intrados. Therefore, the observed differences are here interpreted as compositional differences among selected architectural contexts, possibly related to construction practice, local surface condition and/or restoration history. Further petrographic, stratigraphic and mechanical analyses are required to clarify the relationship between mortar composition and structural function.

(iii) Construction history and technological choices: from the historical-architectural point of view, the analysed ancient mortars are all attributed to the second Roman phase, when the annular corridor was realized by demolishing the lower steps of the *cavea*. The molecular differences observed between podium and vault mortars may therefore reflect distinct functional roles within this intervention or small chronological variations in mortar preparation**.**

(iv) Preliminary vulnerability assessment**:** the discrimination of an endolithic microbe, i.e. *cyanobacteria,* in TY_OU_19, presumably responsible for the biodeteriorative phenomena visible on the surface, represents a first step for the definition of the best pathway for the vulnerability assessment and usability of the investigated site.

(v) Discriminators between modern materials: the nature of the detected individual grains achieved by μ-Raman spectroscopy turned out to be different between the two modern fragments, as expected. In particular, the occurrence of hematite in the molecular composition of TY_OU_1, and of titanium dioxide and silicates in TY_OU_2, allowed us to identify potential compositional markers for sample discrimination, likely related to the different technological choices and restoration strategies involved in their manufacturing/treatment.

Overall, these results underline the importance of integrating spectroscopic analyses with archaeological and architectural information, and represent a fundamental pre-requisite for conservators and restorers when planning future restoration and conservation strategies to be applied.

4. CONCLUSIONS

A preliminary molecular characterization of ancient and modern mortars from the theatre of the archaeological area of Tindari (Sicily, Italy) has been carried out in situ by combining DRIFTS and μ-Raman spectroscopy. The study focuses on five representative areas selected from a broader diagnostic campaign, and should therefore be considered as a case-study evaluation of the potential of the integrated spectroscopic approach.

The combined results allow the investigated ancient and modern areas to be distinguished on the basis of their main mineralogical and molecular features. The ancient mortars attributed to one of the Roman phases show differences among the analysed superficial areas, with quartz- and clay-rich features observed in the podium mortars and a more calcite-related signature in the area investigated on the vaulted annular corridor. However, these differences cannot be interpreted as definitive evidence of functional differentiation without further stratigraphic, mineralogical, and mechanical analyses.

The modern restoration mortars show different spectroscopic features, including phases compatible with conglomerate- and cement-based materials. The detection of hematite in TY_OU_1 and anatase/silicate-related features in TY_OU_2 provides useful local markers for distinguishing the two restoration materials, although no specific technological or functional role is inferred from the present data alone.

The comparison between DRIFTS and μ-Raman spectroscopy confirms the complementarity of the two techniques. DRIFTS averages the signal over a larger superficial area, while μ-Raman provides localized information on individual grains, minor phases and biological colonization. The identification of carotenoid bands in TY_OU_19 suggests the presence of phototrophic biological colonization, which may be relevant for future vulnerability assessment.

From a conservation perspective, the recognition of mineral phases, restoration-related compounds, and possible biodeterioration markers represents a useful preliminary step towards the design of more targeted diagnostic protocols. Further investigations, including X-ray fluorescence (XRF), laser-induced breakdown spectroscopy (LIBS), petrographic observations, and statistical treatment of the complete dataset, will be necessary to establish more robust correlations between mortar composition, construction phases, restoration materials, and degradation patterns.

ACKNOWLEDGEMENT

This research activity was funded by the European Union (NextGeneration EU), through the MUR-PNRR project SAMOTHRACE (ECS00000022) "SiciliAn MicronanOTecH Research And Innovation CEnter" – Ecosistema dell'innovazione (PNRR, Mission 4, Component 2 Investment 1.5, Avviso n. 3277 del 30-12-2021), Spoke 2 – University of Messina – Work Package 6 Cultural Heritage.

REFERENCES

[1] I. Paternò Castello, Viaggio per tutte le antichità di Sicilia, Tipografia di Francesco Abbate, Palermo, 1817, pp. 245–247. [In Italian]

[2] J. Houel, Voyage pittoresque des îles de Sicile, Malte et Lipari, Vol. I, Imprimerie de Monsieur, Paris, 1782. [In French]

[3] M. Panagiotonakou, Revisiting the Theater of Tyndaris: A new chronology proposal, J. Anc. Archit. 2 (2023) pp. 9–30.

[4] H. Bulle, W. Wrede, K. Lehmann, H. Wirsing, H. Möbius, Untersuchungen an griechischen Theatern, Verlag der Bayerischen Akademie der Wissenschaften, München, 1928, tavv. 33–41, pp. 131–152. [In German]

[5] L. Bernabò Brea, Due secoli di studi, scavi e restauri del teatro greco di Tindari, Rivista dell'Istituto nazionale d'archeologia e storia dell'arte 13/14 (1964/1965), pp. 99–144. [In Italian]

[6] P. Cardiano, S. Sergi, C. De Stefano, S. Ioppolo, P. Piraino, Investigations on ancient mortars from the Basilian monastery of Fragalà, J. Therm. Anal. Calorim. 91 (2008), pp. 477–485. DOI: 10.1007/s10973-006-8313-8

[7] C. Gallo, G. M. C. Gemelli, S. Carbone, Y. Caso, M. Sergio, N. Messuti, C. Napoli, E. Caliano, Chemical and mineralogical characterization as a reliable approach for assessing the mechanical properties of ancient mortars and masonry: A case study of the bell tower of Melfi Cathedral (Basilicata, Italy), Acta IMEKO 14 (2025) 4, pp. 1–8.
DOI: 10.21014/actaimeko.v14i4.2128

[8] R. Fort, M. J. Varas-Muriel, D. Ergenç, J. Cassar, M. Anastasi, N. C. Vella, The technology of ancient lime mortars from the Żejtun Roman Villa (Malta), Archaeol. Anthropol. Sci. 15 (2023), p. 15.
DOI: 10.1007/s12520-022-01710-3

[9] M. Jia, G. Wei, C. Grifa, J. Zhang, B. Cui, M. Li, J. Xu, X. Ma, Characterization of archaeological lime mortars in a Ming dynasty tomb: A multi-analytical approach, Archaeometry 65 (2023), pp. 736–753.
DOI: 10.1111/arcm.12855

[10] C. Rispoli, S. F. Graziano, C. Di Benedetto, A. De Bonis, V. Guarino, R. Esposito, V. Morra, P. Cappelletti, New Insights of Historical Mortars Beyond Pompei: The Example of Villa del Pezzolo, Sorrento Peninsula, Minerals 9 (2019), p. 575.
DOI: 10.3390/min9100575

[11] S. E. Spoto, G. Paladini, F. Caridi, V. Crupi, S. D'Amico, D. Majolino, V. Venuti, Multi-Technique Diagnostic Analysis of Plasters and Mortars from the Church of the Annunciation (Tortorici, Sicily), Materials 15 (2022), p. 958.
DOI: 10.3390/ma15030958

[12] I. Marcaida, M. Maguregui, H. Morillas, N. Prieto-Taboada, M. Veneranda, S. Fdez-Ortiz de Vallejuelo, A. Martellone, B. De Nigris, M. Osanna, J. M. Madariaga, In situ non-invasive multianalytical methodology to characterize mosaic tesserae from the House of Gilded Cupids, Pompeii, Herit. Sci. 7 (2019), Art. nr. 3.
DOI: 10.1186/s40494-019-0246-1

[13] O. Gómez-Laserna, P. Cardiano, M. Diez-Garcia, N. Prieto-Taboada, L. Kortazar, M. Á. Olazabal, J. M. Madariaga, Multi-analytical methodology to diagnose the environmental impact suffered by building materials in coastal areas, Environ. Sci. Pollut. Res. 25 (2018), pp. 4371–4386.
DOI: 10.1007/s11356-017-0798-0

[14] J. Couvidat, M. Benzaazoua, V. Chatain, H. Bouzahzah, Environmental evaluation of dredged sediment submitted to a solidification stabilization process using hydraulic binders, Environ. Sci. Pollut. Res. 23 (2016), pp. 17142–17157.
DOI: 10.1007/s11356-016-6869-9

[15] D. P. Da Silva Dalto, R. C. D. C. Ribeiro, L. C. R. De Moura, Characterization of the lime mortars of the Rui Barbosa House Museum in Rio De Janeiro, Brazil, Minerals 8 (2018), p. 50.
DOI: 10.3390/min8020050

[16] M. Sfacteria, S. Tuccinardi, M. Venuti, An integrated approach to the study of the architectural features of the theatre of Tyndaris, Proc. of the IMEKO TC26 Int. Conf. on Metrology for Archaeology and Cultural Heritage, Bergamo, Italy, October 15–17, 2025, pp. 124–128.
DOI: 10.21014/tc26-2025.023

[17] S. Tuccinardi, M. Venuti, Appunti per una rilettura critica del teatro di Tindari, Quaderni di Archeologia, n.s., n. XVI, 2026, pp. 59–83. [In Italian]

[18] I. Arrizabalaga, O. Gómez-Laserna, J. A. Carrero, J. Bustamante, A. Rodríguez, G. Arana, J. M. Madariaga, Diffuse reflectance FTIR database for the interpretation of the spectra obtained with a handheld device on built heritage materials, Anal. Methods 7 (2015), pp. 1061–1070.
DOI: 10.1039/C4AY02189D

[19] A. S. Reichert, A. B. López-Baldomero, F. Moronta-Montero, A. López-Montes, E. M. Valero, C. Cardell, Database of diffuse reflectance infrared Fourier transform spectroscopy (DRIFTS) and hyperspectral imaging (HSI) spectra of pigments and dyes for historical document analysis, Anal. Bioanal. Chem. 417 (2025), pp. 4351–4372.
DOI: 10.1007/s00216-025-05948-3

[20] I. M. Bell, R. J. H. Clark, P. J. Gibbs, Raman spectroscopic library of natural and synthetic pigments (pre-≈1850 AD), Spectrochim.

Acta Part A Mol. Biomol. Spectrosc. 53 (1997), pp. 2159–2179. DOI: 10.1016/S1386-1425(97)00140-6
[21] M. C. Caggiani, A. Cosentino, A. Mangone, Pigments Checker version 3.0, a handy set for conservation scientists: A free online Raman spectra database, Microchem. J. 129 (2016), pp. 123–132. DOI: 10.1016/j.microc.2016.06.020
[22] B. Lafuente, R. T. Downs, H. Yang, N. Stone, The power of databases: The RRUFF project. In Highlights in Mineralogical Crystallography; Armbruster, T., Danisi, R.M., Eds.; W. De Gruyter: Berlin, Germany, 2015, pp. 1–30, ISBN 9783110417104.
[23] J. Madejová, FTIR techniques in clay mineral studies, Vibr. Spectrosc. 31 (2003), pp. 1–10. DOI: 10.1016/S0924-2031(02)00065-6
[24] N. Rovella, A. Arcudi, V. Crupi, M. F. La Russa, D. Majolino, M. Osanna, R. Pace, S. A. Ruffolo, (+ 3 more authors), Tituli Picti in the archaeological site of Pompeii: diagnostic analysis and conservation strategies. Eur. Phys. J. Plus 133 (2018), p. 539. DOI: 10.1140/epjp/i2018-12369-2
[25] H. Yang, A. M. Mouazen, Vis/Near- and Mid- Infrared Spectroscopy for Predicting Soil N and C at a Farm Scale, Infrared Spectroscopy - Life and Biomedical Sciences; InTech, 2012, pp. 1–26.
[26] M. M. Jordán, J. Jordá, F. Pardo, M. A. Montero, Mineralogical Analysis of Historical Mortars by FTIR, Materials 12 (2019), p. 55. DOI: 10.3390/ma12010055
[27] N. Marinoni, M. A. T. M. Broekmans, Microstructure of selected aggregate quartz by XRD, and a critical review of the crystallinity index, Cem. Concr. Res. 54 (2013), pp. 215–225. DOI: 10.1016/j.cemconres.2013.08.007
[28] K. Němečková, J. Mareš, L. Procházková, A. Culka, F. Košek, J. Wierzchos, L. Nedbalová, J. Dudák, V. Tymlová, J. Žemlička, et al., Gypsum endolithic phototrophs under moderate climate (Southern Sicily): their diversity and pigment composition, Front. Microbiol. 14 (2023), pp. 1-21. DOI: 10.3389/fmicb.2023.1175066
[29] V. E. de Oliveira, M. A. C. Neves Miranda, M. C. S. Soares, H. G. M. Edwards, L. F. C. de Oliveira, Study of carotenoids in cyanobacteria by Raman spectroscopy. Spectrochim. Acta Part A Mol. Biomol. Spectrosc. 150 (2015), pp. 373–380. DOI: 10.1016/j.saa.2015.05.044
[30] J. Jehlička, H.G.M. Edwards, A. Oren, Raman Spectroscopy of Microbial Pigments, Appl. Environ. Microbiol. 80 (2014), pp. 3286–3295. DOI: 10.1128/AEM.00699-14
[31] J. Jehlička, A. Culka, L. Mana, A. Oren, Comparison of Miniaturized Raman Spectrometers for Discrimination of Carotenoids of Halophilic Microorganisms, Front. Microbiol. 10 (2019), pp. 1-12. DOI: 10.3389/fmicb.2019.01155
[32] J. Jehlička, H. G. M. Edwards, A. Oren, Bacterioruberin and salinixanthin carotenoids of extremely halophilic Archaea and Bacteria: A Raman spectroscopic study, Spectrochim. Acta Part A Mol. Biomol. Spectrosc. 106 (2013), pp. 99–103. DOI: 10.1016/j.saa.2012.12.081
[33] T. Zhu, X. Lu, M. Dittrich, Calcification on mortar by live and UV-killed biofilm-forming cyanobacterial Gloeocapsa PCC73106, Constr. Build. Mater. 146 (2017), pp. 43–53. DOI: 10.1016/j.conbuildmat.2017.04.026
[34] E. Gallego-Cartagena, H. Morillas, M. Maguregui, K. Patiño-Camelo, I. Marcaida, W. Morgado-Gamero, L. F. O. Silva, J. M. Madariaga, A comprehensive study of biofilms growing on the built heritage of a Caribbean industrial city in correlation with construction materials, Int. Biodeterior. Biodegrad. 147 (2020), 104874. DOI: 10.1016/j.ibiod.2019.104874
[35] T. Zhu, M. L. Merroun, G. Arhonditsis, M. Dittrich, Attachment on mortar surfaces by cyanobacterium Gloeocapsa PCC 73106 and sequestration of CO_2 by microbially induced calcium carbonate, MicrobiologyOpen 10 (2021), e1243. DOI: 10.1002/mbo3.1243
[36] C. A. Crispim, C. C. Gaylarde, Cyanobacteria and Biodeterioration of Cultural Heritage: A Review, Microb. Ecol. 49 (2005), pp. 1–9. DOI: 10.1007/s00248-003-1052-5
[37] K. Hips, J. Haas, Calcimicrobial stromatolites at the Permian–Triassic boundary in a western Tethyan section, Bükk Mountains, Hungary, Sediment. Geol. 185 (2006), pp. 239–253. DOI: 10.1016/j.sedgeo.2005.12.016
[38] M. Stefanidou, P. Koltsou, The Role of Sand in Mortar's Properties, Sand in Construction (2022). IntechOpen. DOI: 10.5772/intechopen.102489
[39] A. Peys, V. Isteri, J. Yliniemi, A. S. Yorkshire, P. N. Lemougna, C. Utton, (+3 more author), Sustainable iron-rich cements: Raw material sources and binder types, Cem. Concr. Res. 157 (2022), p. 106834. DOI: 10.1016/j.cemconres.2022.106834
[40] A. Baral, C. Pesce, A. S. Yorkshire, Z. Zhakiyeva, R. Snellings, T. Hanein, J. L. Provis, A. Peys, Characterisation of iron-rich cementitious materials, Cem. Concr. Res. 177 (2024), p. 107419. DOI: 10.1016/j.cemconres.2023.107419
[41] A. Mancini, B. Lothenbach, G. Geng, D. Grolimund, D. F. Sanchez, S. C. Fakra, (+ 3 more author), Iron speciation in blast furnace slag cements, Cem. Concr. Res. 140 (2021), p. 106287. DOI: 10.1016/j.cemconres.2020.106287
[42] L. Black, Raman spectroscopy of cementitious materials, in: J. Yarwood, R. Douthwaite, S. Duckett (Eds.), Spectroscopic Properties of Inorganic and Organometallic Compounds, Royal Society of Chemistry, Cambridge (2009), pp. 229–249. DOI: 10.1039/b715000h
[43] B. Bergamo, L. de Ferri, A. Cianciosi, S. Gelichi, G. Pojana, Spectroscopic investigation of early medieval tiles and bedding mortars from Nonantola (Modena, Italy) excavations, Eur. Phys. J. Plus 134 (2019), 209. DOI: 10.1140/epjp/i2019-12642-x
[44] S. J. Kelloway, N. Kononenko, R. Torrence, E. A. Carter, Assessing the viability of portable Raman spectroscopy for determining the geological source of obsidian, Vib. Spectrosc. 53 (2010), pp. 88–96. DOI: 10.1016/j.vibspec.2010.02.006
[45] G. Paladini, P. Cardiano, F. Caridi, L. Pistorino, D. Majolino, F. Gregorio, S. Lanza, G. Lando, (+ 4 more authors), Comparative Analysis of Mineralogical Composition and Radioactivity Levels in Stone Samples from the Archaeological Site of Halaesa (Sicily, Italy), Appl. Sci. 15 (2025), p. 5915. DOI: 10.3390/app15115915